Metallic and superconducting gallane under high pressure

Guoying Gao,[1] Hui Wang,[1] Aitor Bergara,[2,3,4] Yinwei Li,[1] Guangtao Liu,[1] and Yanming Ma[1,*]

[1]*State Key Lab of Superhard Materials, Jilin University, Changchun 130012, P. R. China*

[2]*Materia Kondentsatuaren Fisika Saila, Zientzia eta Teknologia Fakultatea, Euskal Herriko Unibertsitatea, 644 Postakutxatila, 48080 Bilbo, Basque Country, Spain*

[3]*Donostia International Physics Center (DIPC), Paseo de Manuel Lardizabal, 20018, Donostia, Basque Country, Spain*

[4]*Centro de Fisica de Materiales CSIC-UPV/EHU, 1072 Posta kutxatila, E-20080 Donostia, Basque Country, Spain*

(Received 15 May 2011; revised manuscript received 6 July 2011; published 24 August 2011)

Using our newly developed particle swarm optimization algorithm on crystal structural prediction, we characterized the pressure-induced structural transition sequence of gallane (GaH_3). As has been observed in alane (AlH_3), enthalpy calculations reveal that the $Pm\bar{3}n$ structure of GaH_3 becomes stable above 160 GPa, below which it is unstable with respect to elemental decomposition. Interestingly, the $Pm\bar{3}n$ structure is metallic, and the application of the Allen-Dynes modified McMillan equation reveals a high superconducting transition temperature (T_c), which reaches 86 K at 160 GPa and increases with decreasing pressure (T_c = 102 K at 120 GPa). Our band structure calculations demonstrate that GaH_3 within the $Pm\bar{3}n$ structure is a highly ionic solid, where the ionicity of H atoms plays an important role in the predicted high temperature superconductivity.

DOI: 10.1103/PhysRevB.84.064118 PACS number(s): 74.70.Ad, 74.10.+v, 74.25.Jb, 74.62.Fj

I. INTRODUCTION

Long ago, Ashcroft predicted that metallic hydrogen might be a high-temperature superconductor;[1] however, pressure-induced metallic transition of hydrogen is still an elusive goal of physics, even at pressures around 300 GPa.[2–4] Recently, it has been proposed that hydrogen-rich compounds, such as group IVa hydrides (SiH_4, GeH_4, and SnH_4), might become metallic at lower pressures than hydrogen and might well be superconductors with high critical temperatures.[5] Although the metallicity and superconductivity experimentally observed in SiH_4 under pressure[6,7] were actually attributed to the formation of PtH and Si,[8,9] its metallization pressure was predicted to be lower than in solid hydrogen.[10,11] Our previous work also suggested that GeH_4[12,13] and SnH_4[14] might metallize and become good superconductors at experimentally accessible pressures. These results are sufficiently encouraging to prompt further studies of a wider range of hydrides.

Due to its potential application as a hydrogen storage material, alane (AlH_3) has recently been the subject of many theoretical and experimental investigations.[15,16] Using a "random searching" technique, Pickard *et al.*[16] predicted a metallic cubic phase (space group $Pm\bar{3}n$) for high-pressure AlH_3. Subsequently, Goncharenko *et al.*[15] indeed observed that AlH_3 becomes metallic at 100 GPa and confirmed the predicted structure. However, no superconducting transition was found down to 4 K, which disagrees with the theoretically estimated T_c of ∼20 K.[15] The origin for this disagreement between theory and experiment was explained by the high anharmonic renormalization of selected phonon modes inducing the superconducting transition, which considerably decreased the electron-phonon coupling parameter λ.[17] Considering the larger polarizability of GaH_3 compared to AlH_3, according to the Goldhammer-Herzfeld criterion,[18] GaH_3 should be a good candidate to metallize at even lower pressures. In this article, we apply our newly developed particle swarm optimization (PSO) technique on crystal structure prediction[19] to extensively explore the crystal structures of GaH_3 under high pressure and characterize the electronic, dynamical, and superconducting properties of the predicted high-pressure structures.

II. COMPUTATIONAL DETAILS

The crystal structure prediction is based on a global minimization of free-energy surfaces merging *ab initio* total-energy calculations via PSO technique as implemented in the Crystal structure AnaLYsis by Particle Swarm Optimization (CALYPSO) code.[19] This methodology has been successfully applied to many high-pressure structures on elemental, binary, and ternary compounds with metallic, ionic, and covalent bondings.[19–22] The underlying *ab initio* structural relaxations were performed using density functional theory within the Perdew-Burke-Ernzerh (PBE) parameterization of the generalized gradient approximation (GGA)[23] as implemented in the Vienna *ab initio* Simulation Package (VASP) code.[24] The all-electron projector-augmented wave (PAW) method[25] was adopted with the PAW potentials, where 1*s* and 3*d*4*s*4*p* are treated as valence electrons for H and Ga atoms, respectively. A plane-wave basis set with an energy cutoff of 800 eV was used to get well-converged total energies. On the other hand, the plane-wave pseudopotential method within the PBE-GGA as implemented in the Quantum-ESPRESSO package[26] was used to characterize the electronic properties, lattice dynamics, and electron-phonon coupling (EPC) for $Pm\bar{3}n$ GaH_3. For these purposes, ultrasoft pseudopotentials for H and Ga were considered, and convergence tests concluded that suitable values would be a 100 Ry kinetic energy cutoff and a 12 × 12 × 12 Monkhorst-Pack (MP)[27] *k*-point sampling mesh for the electronic Brillouin zone (BZ) integration. Phonon frequencies were calculated based on the density functional linear-response theory,[28] and a 4 × 4 × 4 *q*-mesh in the first BZ was used in the interpolation of the force constants for the phonon dispersions. The EPC spectral function $\alpha^2F(\omega)$ can be expressed in terms of the phonon linewidth γ_{qj}, owing to electron-phonon scattering,[29–31]

$$\alpha^2F(\omega) = \frac{1}{2\pi N_f}\sum_{qj}\frac{\gamma_{qj}}{\omega_{qj}}\delta(\hbar\omega - \hbar\omega_{qj}), \qquad (1.1)$$

where N_f is the electronic density of states per atom and spin at the Fermi level. The linewidth of a phonon mode j at wave vector q, γ_{qj}, arising from electron-phonon interaction is given by

$$\gamma_{qj} = 2\pi\omega_{qj} \sum_{knm} \left|g^j_{kn,k+qm}\right|^2 \delta(\varepsilon_{kn})\delta(\varepsilon_{k+qm}), \qquad (1.2)$$

where the sum is over the BZ, and ϵ_{kn} are the energies of bands measured with respect to the Fermi level at point k, and $g^j_{kn,k+qm}$ is the electron-phonon matrix element. The EPC parameter λ can be defined as the first reciprocal moment of the spectral function $\alpha^2F(\omega)$,

$$\lambda = 2\int_0^\infty \frac{\alpha^2F(\omega)}{\omega} d\omega \approx \sum_{qj} \lambda_{qj}\omega(q), \qquad (1.3)$$

where $\omega(q)$ is the weight of a q point in the first BZ. We substituted a Gaussian for the δ function in Eq. (1.2). The superconducting transition temperature T_c has been estimated with the Allen-Dynes modified McMillan equation as[32]

$$T_C = \frac{\omega_{\log}}{1.2} \exp\left[-\frac{1.04(1+\lambda)}{\lambda - \mu^*(1+0.62\lambda)}\right], \qquad (1.4)$$

where $\omega_{\log}$ is the logarithmic average frequency, and μ^* is the Coulomb pseudopotential. An MP grid of $20 \times 20 \times 20$ was used to ensure k-point sampling convergence with Gaussians of width 0.04 Ry, in order to approximate the zero-width limit in the calculations of the EPC parameter, λ.

III. RESULTS AND DISCUSSIONS

Structural predictions were performed with the CALYPSO code, considering simulation sizes ranging from one to four GaH_3 formula units (f.u.) at 5, 50, 100, 200, and 300 GPa. The predicted stable structures were then carefully optimized at a higher level of accuracy at other pressure points for enthalpy curve and electron-phonon coupling calculations. Before the structural searches converged to the most stable structures, we typically generated several hundred structures (e.g., at 300 GPa simulation, we need 100–400 structures to derive the most stable structure of $Pm\bar{3}n$). For example, according to our simulations, the structure with the lowest enthalpy at 5 GPa is the base centered monoclinic Cc structure (2 formula units/unit cell, f.u./cell), and at 50 and 100 GPa, we observed that the simple monoclinic $P2_1/m$ phase (4 f.u./cell) becomes the preferred one [see Figs. 1(a) and 1(b)]. The existence of semimolecular H_2 in the Cc and $P2_1/m$ structures demonstrates the decomposition trend for GaH_3 at low pressure. In addition, two metastable hexagonal phases (6 f.u./cell) with space groups $R\bar{3}c$ and $P6_322$, which are very similar to the low-pressure structure of AlH_3, built from AlH_6 octahedrons linked by Al-H-Al bridges,[16] are also predicted at 5 GPa. Finally, at 200 and 300 GPa, a cubic structure of the space group $Pm\bar{3}n$ [Fig. 1(c)] is predicted. This structure is characterized by two aluminum atoms located at a simple body centered cubic lattice and equivalent H atoms forming chains running along each Cartesian direction. Interestingly, the same structure has also been observed in high-pressure AlH_3. The nearest H-H distance at 160 GPa is 1.547 Å, which is much longer than the H-H bonding length of ~1.2 Å and shorter than the Ga-H distance of 1.73 Å. Moreover, H-H distances decrease very slowly with increasing pressure and become 1.458 Å at 300 GPa, showing that H atoms do not present any bonding trend.

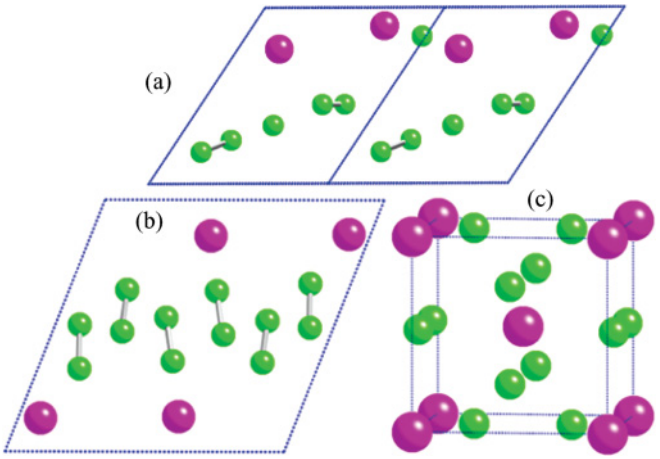

FIG. 1. (Color online) Predicted (a) Cc, (b) $P2_1/m$, and (c) $Pm\bar{3}n$ structures for GaH_3. Gallium atoms are shown in pink, and hydrogen atoms are shown in green. The $Pm\bar{3}n$ structure contains 2 f.u. for each cell, gallium atoms occupy the crystallographic $2a$ (0, 0, 0) site, and hydrogen atoms are located at the $6c$ (0.5, 0.25, 0) site.

The enthalpy curves of our predicted structures relative to $R\bar{3}c$ as a function of pressure are presented in Fig. 2. It is clearly seen that below 182 GPa GaH_3 is thermodynamically unstable with respect to decomposition of its elements. Actually, AlH_3 is also thermodynamically unstable at standard temperature and pressure, and it releases H_2 molecules under moderate heating.[16,33] Above 182 GPa, the $Pm\bar{3}n$ structure clearly becomes the most stable structure. Considering the low mass

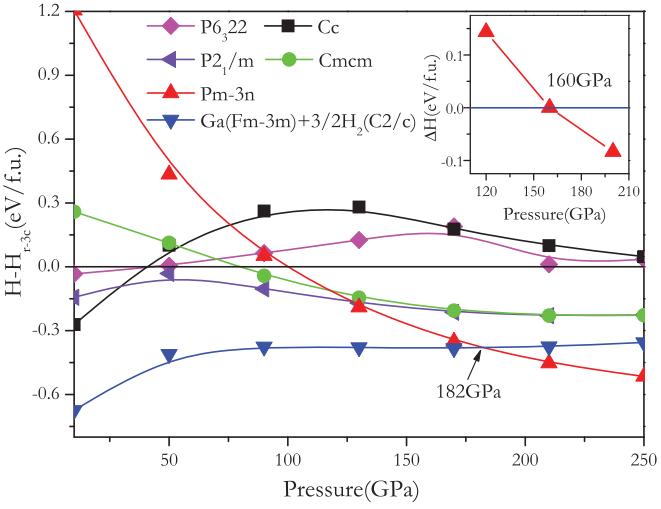

FIG. 2. (Color online) The enthalpies per formula unit of various structures as a function of pressure with respect to $R\bar{3}c$ structure. The decomposition ($Ga + 3/2H_2$) enthalpies are calculated by adopting the $C2/c$ structure for H_2[39] and $Cmca$, $I4/mmm$, $Fm\bar{3}m$, and $R\bar{3}c$ structures for Ga,[40] respectively. Inset: Enthalpies for the $Pm\bar{3}n$ structure relative to the decomposition ($Fm\bar{3}m$-Ga + $C2/c$-H_2) with the zero-point corrections.

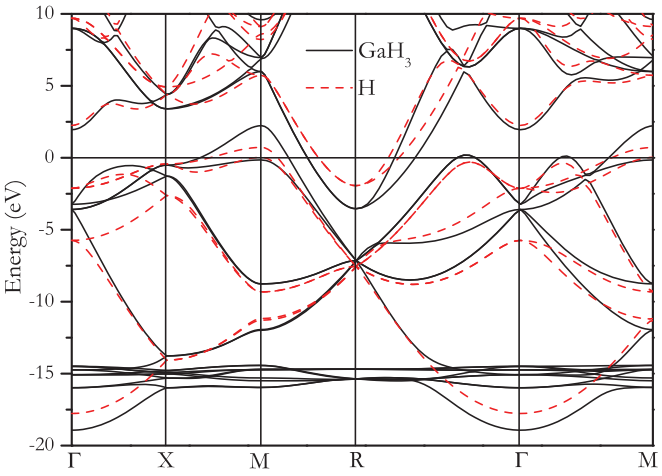

FIG. 3. (Color online) Calculated electronic band structures (full black line) for $Pm\bar{3}n$ GaH_3 at 160 GPa compared with the hypothetical system composed of the hydrogen subsystem immersed in a jellium background (dashed red line).

of H atoms, we applied the quasiharmonic approximation[34] to estimate the zero-point (ZP) energies of GaH_3, Ga, and H_2 at 120, 160, and 200 GPa. Interestingly, the inclusion of ZP energies lowers the stabilization pressure of $Pm\bar{3}n$ to 160 GPa.

Motivated by the search for metallic and high superconducting T_c, hydrogen-rich compounds within the reach of current experimental techniques, the electronic properties, lattice dynamics, and superconductivity of the $Pm\bar{3}n$ structure at 160 GPa were also analyzed. Figure 3 presents the calculated electronic band structure for $Pm\bar{3}n$ GaH_3 at 160 GPa. The overlap between the conduction and the valence bands under pressure makes $Pm\bar{3}n$ GaH_3 a metal. As can be seen in the ΓR and ΓM directions, two maxima in the band structure at k-points close to Γ are located at the Fermi level, and they make GaH_3 have much larger density of states (DOS) at the Fermi energy (3.1×10^{-2} states/eV/Å^3) than our calculated data in AlH_3 (1.1×10^{-2} states/eV/Å^3 at 80 GPa).

In order to understand the role of H atoms in GaH_3, we also analyzed the band structure of a hypothetical system composed of only the hydrogen sublattice and a compensating background charge ("hydrogen subsystem"). As can be seen in Fig. 3, the band structures of GaH_3 and the hydrogen subsystem are qualitatively similar, which basically indicates that the introduction of Ga atoms does not strongly affect the band structure of the hydrogen sublattice. Therefore, the main role of Ga atoms in GaH_3 is to donate electrons that go to H-like bands, and Ga associated bands remain unoccupied. The charge transfer from Ga to H atoms indicates a strong ionic character of GaH_3, similar to those in AlH_3 and LiH_n.[16,35] Compared with the behavior observed in AlH_3,[36] near the Fermi energy, the presence of Ga atoms notably shifts the bands down at the R point and slightly up at M. In the absence of Ga atoms, the electronic charge associated to states at R piles up around gallium sites; however, when Ga atoms are present, the density profile is highly modified. As is shown in Fig. 4, electronic states at R become highly localized around Ga atoms, and this lowers the energy associated with these states when compared to the hydrogen subsystem, which explains the previously mentioned energy shift in the band structure at R. The strong ionic character for H atoms in $Pm\bar{3}n$ GaH_3 is different from group IV hydrides (i.e., SiH_4, GeH_4, and SnH_4), where the H atoms are either bonded to the nearest H atoms to form semimolecular H_2, and/or they are covalently bonded to M (M = Si, Ge, or Sn) atoms to form M-H bonds. Interestingly, the high-pressure phase ($Pm\bar{3}m$) of Si_2H_6 also has H atoms with a strong ionic character, which has shown to favor the superconducting transition characterized by a predicted high

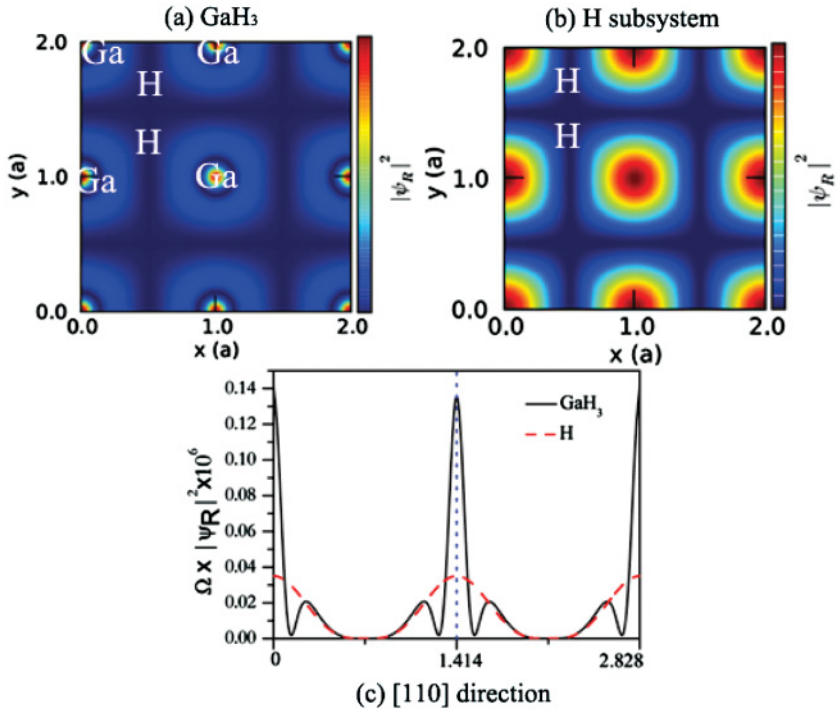

FIG. 4. (Color online) Electronic density contribution from states at the R point close to the Fermi energy for $Pm\bar{3}n$ GaH_3 at 160 GPa, showing the density on the (100) plane for GaH_3 (a) and for the hydrogen system (b). Comparison of the densities in the [110] direction is also shown (c). The vertical lines indicate the positions of the Ga sites. Many periodic repetitions are shown for clarity.

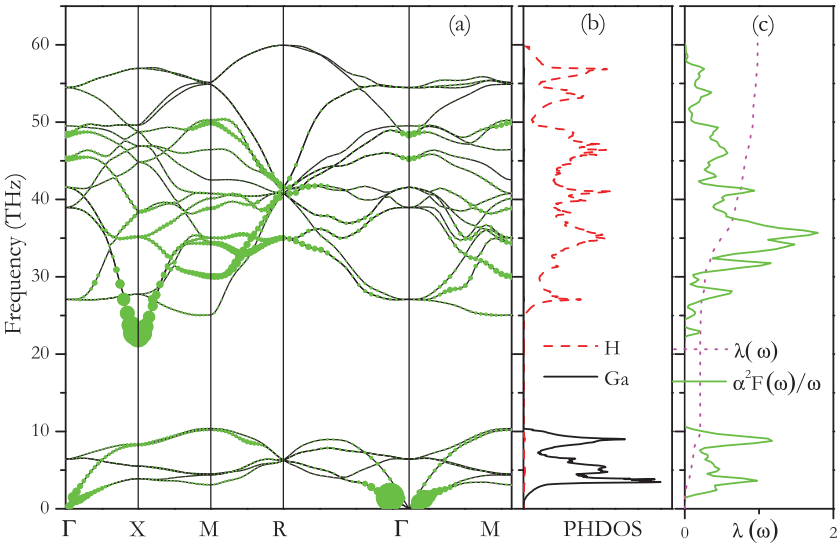

FIG. 5. (Color online) (a) Calculated phonon band structure for $Pm\bar{3}n$ GaH_3 at 160 GPa. Green solid circles show the electron-phonon coupling with the radius proportional to their respective strength. The Eliashberg phonon spectral function, $\alpha^2F(\omega)$, and the partial electron-phonon integral, $\lambda(\omega)$, in (c) are compared to the phonon DOS projected on Ga and H atoms in (b).

T_c of ~130 K.[37] Therefore, we expect that the same trend might also be observed in $Pm\bar{3}n$ GaH_3. The absence of any imaginary frequency phonon modes [see Fig. 5(a)] proves the dynamical stability of the $Pm\bar{3}n$ structure within the studied pressure range. As can be seen in Fig. 5(b), the low-energy phonon modes, with frequencies below 11 THz, are mainly associated with Ga atoms, as expected from their much higher atomic mass, while modes with higher frequencies correspond to H atoms.

To explore the superconducting properties, we calculated the electron-phonon coupling (EPC) parameter, λ, the logarithmic average phonon frequency, $\omega_{\ln}$, and the electronic DOS at the Fermi level, $N(E_f)$, at several pressures (Table I). According to our calculations, at 160 GPa, λ reaches 0.98, and $\omega_{\ln}$ is 1271 K, so that the estimated T_c becomes 76–83 K, considering typical Coulomb pseudopotential parameters, μ^*, of 0.13 and 0.1, respectively. The large T_c in the $Pm\bar{3}n$ structure is mainly attributed to the strong electron phonon coupling, λ, and the high $\omega_{\log}$. In order to understand the origin of this strong λ, we also calculated the Eliashberg phonon spectral function, $\alpha^2F(\omega)/\omega$, and the partial electron-phonon integral, $\lambda(\omega)$. As can be seen in Fig. 5(c), although compressed AlH_3 and GaH_3 share the same structure, the resulting Eliashberg phonon spectral functions are quite different. Contrary to AlH_3,[15,17] the main contribution to λ in GaH_3 is not associated with phonons around just two modes at the X point. Similar to the group IVa hydrides,[12–14] in GaH_3 there is an overall contribution of different modes to λ, and the contribution associated with the previously mentioned two modes around X becomes negligible [Fig. 5(c)]. Therefore, we also expect that the predicted anharmonic renormalization for AlH_3[17] of these two modes at X will not affect the calculated T_c in GaH_3. Note that the low-frequency vibrations provide a contribution of 25% of the total EPC parameter, while the phonon frequencies between 30–40 THz account for nearly 50% of λ. To further explore the contribution associated with different phonon modes, solid circles with the radius proportional to the electron-phonon coupling are also plotted in Fig. 5(a). Interestingly, phonon modes between 30 and 36 THz along M-R are primarily responsible for the main peak in the Eliashberg phonon spectral function, $\alpha^2F(\omega)/\omega$, and give an important contribution to λ. Moreover, these phonon modes are mainly associated with the vibrations of ionic H. Under pressure, all the phonon modes and the spectral function shift to higher energy, and the major contribution of the intermediate phonon modes to λ remains. With increasing pressure, the calculated λ and the resulting T_c decrease down to 60 K at 240 GPa. However, λ is predicted to increase up to 1.19 when pressure decreases to 120 GPa, which is the same value as in the $Cmca$ structure for solid hydrogen at 428 GPa.[38] As is shown in Table I, although the calculated $\omega_{\ln}$ lowers with decreasing pressure, reaching 1158 K at 120 GPa, the resulting T_c is predicted to increase up to 102 K, and becomes higher than group IV hydrogen-rich compounds.

In summary, theoretical calculations reveal that a metallic cubic structure for GaH_3 is stable at high pressures

TABLE I. The calculated phonon frequency logarithmic average ($\omega_{\ln}$), EPC parameter (λ), the electronic DOS at Fermi level $N(E_f)$, and critical temperature T_c ($\mu^* = 0.1$ and 0.13) at 120, 160, 200, and 240 GPa, respectively.

P(GPa)	Lambda (λ)	$\omega_{\ln}$ (K)	$N(E_f)$ states/Spin/Ry/cell	T_c (K) with $\mu^* = 0.1$, 0.13	
120	1.19	1158	6.65	102	91
160	0.98	1271	6.13	86	73
200	0.85	1349	5.70	72	59
240	0.76	1407	5.33	60	48

(>160 GPa) against the remarkably high decomposition trend at lower pressures. Electron-phonon coupling calculations show that the $Pm\bar{3}n$ phase of GaH_3 is superconducting with a high T_c of 73–86 K at 160 GPa, and even a much higher T_c of 102 K might be expected at 120 GPa. Our results demonstrate that hydrogen-rich compounds with H atoms of ionic character might have a higher T_c than those with H bonded to metal atoms and/or those forming semimolecular H_2, supporting the conjecture that hydrogen-rich compounds provide a way to achieve a metallic and superconducting phase at accessible experimental pressures.

ACKNOWLEDGMENTS

We acknowledge funding support from the National Natural Science Foundation of China (under Grants No. 91022029 and No. 11025418), the research fund of Key Laboratory of Surface Physics and Chemistry (No. SPC201103), and the China 973 Program under Grant No. 2011CB808204. A.B. acknowledges the Department of Education, Universities and Research of the Basque Government, UPV/EHU (Grant No. IT-366-07), and the Spanish Ministry of Science and Innovation (Grant No. FIS2010-19609-C02-00).

*mym@jlu.edu.cn

[1] N. W. Ashcroft, Phys. Rev. Lett. **21**, 1748 (1968).

[2] P. Loubeyre, F. Occelli, and R. LeToullec, Nature **416**, 613 (2002).

[3] A. F. Goncharov, E. Gregoryanz, R. J. Hemley, and H. K. Mao, Proc. Natl. Acad. Sci. USA **98**, 14234 (2001).

[4] C. Narayana, H. Luo, J. Orloff, and A. L. Ruoff, Nature **393**, 46 (1998).

[5] N. W. Ashcroft, Phys. Rev. Lett. **92**, 187002 (2004).

[6] X. J. Chen, V. V. Struzhkin, Y. Song, A. F. Goncharov, M. Ahart, Z. Liu, H.-k. Mao, and R. J. Hemley, Proc. Natl. Acad. Sci. USA **105**, 20 (2008).

[7] M. I. Eremets, I. A. Trojan, S. A. Medvedev, J. S. Tse, and Y. Yao, Science **319**, 1506 (2008).

[8] M. Hanfland, J. E. Proctor, C. L. Guillaume, O. Degtyareva, and E. Gregoryanz, Phys. Rev. Lett. **106**, 095503 (2011).

[9] O. Degtyareva, J. E. Proctor, C. L. Guillaume, E. Gregoryanz, and M. Hanfland, Solid State Commun. **149**, 1583 (2009).

[10] M. Martinez-Canales, A. R. Oganov, Y. Ma, Y. Yan, A. O. Lyakhov, and A. Bergara, Phys. Rev. Lett. **102**, 087005 (2009).

[11] C. J. Pickard and R. J. Needs, Phys. Rev. Lett. **97**, 045504 (2006).

[12] G. Gao, A. R. Oganov, A. Bergara, M. Martinez-Canales, T. Cui, T. Iitaka, Y. Ma, and G. Zou, Phys. Rev. Lett. **101**, 107002 (2008).

[13] M. Martinez-Canales, A. Bergara, J. Feng, and W. Grochala, J. Phys. Chem. Solids **67**, 2095 (2006).

[14] G. Gao, A. R. Oganov, P. Li, Z. Li, H. Wang, T. Cui, Y. Ma, A. Bergara, A. O. Lyakhov, T. Iitaka, and G. Zou, Proc. Natl. Acad. Sci. USA **107**, 1317 (2010).

[15] I. Goncharenko, M. I. Eremets, M. Hanfland, J. S. Tse, M. Amboage, Y. Yao, and I. A. Trojan, Phys. Rev. Lett. **100**, 045504 (2008).

[16] C. J. Pickard and R. J. Needs, Phys. Rev. B **76**, 144114 (2007).

[17] B. Rousseau and A. Bergara, Phys. Rev. B **82**, 104504 (2010).

[18] K. F. Herzfeld, Phys. Rev. **29**, 701 (1927).

[19] Y. Wang, J. Lv, L. Zhu, and Y. Ma, Phys. Rev. B **82**, 094116 (2010); [http://nlshm-lab.jlu.edu.cn/~calypso.html].

[20] P. Li, G. Gao, Y. Wang, and Y. Ma, J. Phys. Chem. C **114**, 21745 (2011).

[21] J. Lv, Y. Wang, L. Zhu, and Y. Ma, Phys. Rev. Lett. **106**, 015503 (2011).

[22] L. Zhu, H. Wang, Y. Wang, J. Lv, Y. Ma, Q. Cui, Y. Ma, and G. Zou, Phys. Rev. Lett. **106**, 145501 (2011).

[23] J. P. Perdew, K. Burke, and M. Ernzerhof, Phys. Rev. Lett. **77**, 3865 (1996).

[24] G. Kresse and J. Furthmüler, Phys. Rev. B **54**, 11169 (1996).

[25] P. E. Blöhl, Phys. Rev. B **50**, 17953 (1994).

[26] P. Giannozzi, S. Baroni, N. Bonini, M. Calandra, R. Car, C. Cavazzoni, D. Ceresoli, G. L. Chiarotti, M. Cococcioni, I. Dabo, A. D. Corso, S. de Gironcoli, S. Fabris, G. Fratesi, R. Gebauer, U. Gerstmann, C. Gougoussis, A. Kokalj, M. Lazzeri, L. Martin-Samos, N. Marzari, F. Mauri, R. Mazzarello, S. Paolini, A. Pasquarello, L. Paulatto, C. Sbraccia, S. Scandolo, G. Sclauzero, A. P. Seitsonen, A. Smogunov, P. Umari, and R. M. Wentzcovitch, J. Phys. Condens. Matter **21**, 395502 (2009).

[27] H. J. Monkhorst and J. D. Pack, Phys. Rev. B **13**, 5188 (1976).

[28] S. Baroni, S. de Gironcoli, A. Dal Corso, and P. Giannozzi, Rev. Mod. Phys. **73**, 515 (2001).

[29] P. B. Allen and R. Silberglitt, Phys. Rev. B **9**, 4733 (1974).

[30] P. B. Allen, Phys. Rev. B **6**, 2577 (1972).

[31] J. R. Schrieffer, *The Theory of Superconductivity* (Benjamin, New York, 1964).

[32] P. B. Allen and R. C. Dynes, Phys. Rev. B **12**, 905 (1975).

[33] G. C. Sinke, L. C. Walker, F. L. Oetting, and D. R. Stull, J. Chem. Phys. **47**, 2759 (1967).

[34] Y. M. Ma and J. S. Tse, Solid State Commun. **143**, 161 (2007).

[35] E. Zurek, R. Hoffmann, N. W. Ashcroft, A. R. Oganov, and A. O. Lyakhov, Proc. Natl. Acad. Sci. USA **106**, 17640 (2009).

[36] I. G. Gurtubay, B. Rousseau, and A. Bergara, Phys. Rev. B **82**, 085113 (2010).

[37] X. Jin, X. Meng, Z. He, Y. Ma, B. Liu, T. Cui, G. Zou, and H.-k. Mao, Proc. Natl. Acad. Sci. USA **107**, 9969 (2010).

[38] L. Zhang, Y. Niu, Q. Li, T. Cui, Y. Wang, Y. Ma, Z. He, and G. Zou, Solid State Commun. **141**, 610 (2007).

[39] C. J. Pickard and R. J. Needs, Nature Phys. **3**, 473 (2007).

[40] M. I. McMahon and R. J. Nelmes, Chem. Soc. Rev. **35**, 943 (2006).